Biofabrication

International Society for Biofabrication

ACCEPTED MANUSCRIPT

Numerical and experimental simulation of a dynamic-rotational 3D cell culture for stratified living tissue models

To cite this article before publication: Raphael F Canadas *et al* 2022 *Biofabrication* in press https://doi.org/10.1088/1758-5090/ac55a2

Manuscript version: Accepted Manuscript

Accepted Manuscript is “the version of the article accepted for publication including all changes made as a result of the peer review process, and which may also include the addition to the article by IOP Publishing of a header, an article ID, a cover sheet and/or an ‘Accepted Manuscript’ watermark, but excluding any other editing, typesetting or other changes made by IOP Publishing and/or its licensors”

This Accepted Manuscript is **© 2022 IOP Publishing Ltd**.

During the embargo period (the 12 month period from the publication of the Version of Record of this article), the Accepted Manuscript is fully protected by copyright and cannot be reused or reposted elsewhere.
As the Version of Record of this article is going to be / has been published on a subscription basis, this Accepted Manuscript is available for reuse under a CC BY-NC-ND 3.0 licence after the 12 month embargo period.

After the embargo period, everyone is permitted to use copy and redistribute this article for non-commercial purposes only, provided that they adhere to all the terms of the licence https://creativecommons.org/licences/by-nc-nd/3.0

Although reasonable endeavours have been taken to obtain all necessary permissions from third parties to include their copyrighted content within this article, their full citation and copyright line may not be present in this Accepted Manuscript version. Before using any content from this article, please refer to the Version of Record on IOPscience once published for full citation and copyright details, as permissions will likely be required. All third party content is fully copyright protected, unless specifically stated otherwise in the figure caption in the Version of Record.

View the article online for updates and enhancements.

This content was downloaded from IP address 193.60.238.99 on 21/02/2022 at 15:55

Numerical and experimental simulation of a dynamic-rotational 3D cell culture for stratified living tissue models

Raphaël F. Canadas[1,2,3,5ł*], Ziyu Liu[3,4ł],Luca Gasperini[1,2], Diogo C. Fernandes[1,2], Fátima R. Maia[1,2], Rui L. Reis[1,2], Alexandra P. Marques[1,2], Chaozong Liu[3*], Joaquim M. Oliveira[1,2*]

[1] 3B's Research Group, I3Bs – Research Institute on Biomaterials, Biodegradables and Biomimetics, University of Minho, Headquarters of the European Institute of Excellence on Tissue Engineering and Regenerative Medicine, AvePark, Zona Industrial da Gandra, 4805-017 Barco GMR, Portugal;

[2] ICVS/3B's - PT Government Associate Laboratory, Braga/Guimarães, Portugal;

[3] Division of Surgery and Interventional Science, University College London, Royal National Orthopaedic Hospital, London HA7 4LP, United Kingdom;

[4] School of Medical Science and Engineering, Beihang University, Beijing, China.

[5] Tech4MED™, UPTEC, ASPRELA I, Office-Lab 0.16, Business Campus, n.° 455/461, 4200-135 Porto, Portugal

[ł] Contributed equally to this work

*Correspondence should be addressed to:

Raphael F. Canadas (raphael.canadas@tech4med.pt); Joaquim M. Oliveira (miguel.oliveira@i3bs.uminho.pt); Chaozong Liu (chaozong.liu@ucl.ac.uk)

Keywords: Bioreactor; Mathematical model; Tissue engineering; Blood-brain-barrier model; Drug discovery

Accepted Manuscript

Abstract

Human tissues and organs are inherently heterogeneous, and their functionality is determined by the interplay between different cell types, their secondary architecture, and gradients of signalling molecules and metabolites. To mimic the dynamics of native tissues, perfusion bioreactors and microfluidic devices are widely used in tissue engineering (TE) applications for enhancing cell culture viability in the core of 3D constructs. Still, most *in vitro* screening methods for compound efficacy and toxicity assessment include cell or tissue exposure to constant and homogeneous compound concentrations over a defined testing period. Moreover, a prevalent issue inhibiting the large-scale adoption of microfluidics and bioreactor is the tubing dependence to induce a perfusion regime. Here, we propose a compartmentalized rotational (CR) 3D cell culture platform for a stable control over gradient tissue culture conditions. Using the CR bioreactor, adjacent lanes of constructs are patterned by controlled flow dynamics to enable tissue stratification. Numerical and experimental simulation demonstrate cell seeding dynamics, as well as culture media rotational perfusion and gradient formations. Additionally, the developed system induces vertical and horizontal rotations, which increase medium exchange and homogeneous construct maturation, allowing both perfused tubing-based and tubing-free approaches. As a proof-of-concept, experiments and accompanying simulation of cellular inoculation and growth in 3D scaffold and hydrogel were performed, before the examination of a blood-brain-barrier (BBB) model, demonstrating the impact of a heterotypic culture on molecular permeability under mimetic dynamic conditions. Briefly, the present work discloses simulation of 3D dynamic cultures, and a semi-automated platform for heterotypic tissues *in vitro* modelling, for broad tissue engineering and drug discovery/screening applications.

Accepted Manuscript

1. Introduction

The key to understanding and harnessing natural biological processes for TE and modelling lies in providing a controllable dynamic environment for tissue maturation *in vitro*[1]. Furthermore, engineered biological tissues' availability represents an urgent need for clinical applications and basic research in life science laboratories[2].

TE techniques typically make use of constructs, using 3D polymeric scaffolds or hydrogels together with one or more cell types, to create implantable and *in vitro* tissue-like devices or models to replace damaged tissue while replicating specific phenotypic conditions[3]. Engineered tissue models serve as platforms to study normal and diseased biological processes at the tissue level[4]. Moreover, TE strategies aiming at enhancing tissue regeneration and modelling are anticipated to become a regular clinical treatment and drug discovery platform in the future[5], respectively. However, a consensus has yet to be reached about fast, clean, and reproducible procedures to mature tissue constructs towards stratified and interfaced phenotypes for both applications.

In vitro, cells cannot survive when tissue dimensions grow beyond several hundred microns because of diffusive limitations[1]. Thus, perfusion bioreactors play an essential role in creating specific culture conditions necessary for developing 3D engineered tissues by improving nutrient transportation, waste removal and generating mechanical stimulation in the form of shear stress[6]. Direct perfusion culture has already shown beneficial effects for culturing various forms of engineered tissues, such as cardiac[7], hepatic[8], cartilage[9], bone[10], or interfaced tissues[11] with even low flow rates inducing widespread changes in the gene[12] and protein[13] expression levels using multiple cell types. Recently, even an interstitial-like, flow-induced, low, and constant shear stress showed to boost vascular network formation and maturation in a 3D-engineered tissues[14,15].

Although 3D culturing under dynamic conditions was proven to better mimic the natural tissue environment and viability, the overwhelming majority of *in vitro* dynamic systems relies on additional equipment, such as tubing and pumps, reducing the convenience of handling and increasing the risk for contaminations. Besides, microfluidic and bioreactor devices serving as perfusion platforms are still limited in geometry and scale, involving complicated fabrication techniques, assembling methods, and unusually large amounts of tubing, which are factors that increase the technical labour demand and also the chances for leakage and contaminations[1]. Furthermore, most microfluidic and bioreactor devices

Accepted Manuscript

are not conceptualized to serve as both TE and drug screening platforms in stratified tissues or even friendly systems to set up. Thus, direct flow bioreactors are currently the ultimate systems for cultivating clinically relevant engineered tissues but are unsuitable for drug screening studies, control over multiple cell phenotypes in a single environment, and simultaneously not user-friendly nor scalable[6].

Hence, we developed a compartmentalized rotational (CR) 3D cell culture platform for stratified living tissue modelling. The design of the CR bioreactor allows to load up to twelve 3D constructs in its pilot version allowing cell culture under several flow stimulations. The transparent cell culture chamber is compatible with a standard microscope for image screenings, which can be used to study cell dynamics.

In this study, the CR bioreactor is applied to generate 3D-engineered BBB cultured under natural flow conditions. The platform is first tested to form stratified cell cultures in 3D, as verified through computational simulation and the experimental testing, testing cell seeding and using vertical and horizontal rotations. The formation of a heterotypic cellular environment of an endothelial layer interfaced with a 3D neural construct made a 3D dynamic BBB model. The permeability of the endothelial layer is assessed under monoculture and co-culture conditions, as a proof of concept.

Accepted Manuscript

2. Experimental section

2.1. Materials

Polycaprolactone (PCL filament, MakerBot, USA) was used to 3D print the prototyped scaffolds with 500 µm pore size, and poly-lactic acid (PLA filament, MakerBot, USA) was applied to build the backbone of the prototyped rotational platform, both using a MakerBot Replicator 2 (MakerBot Industries LLC, USA). Low Acyl Gellan Gum (LAGG; Gelzan™, molecular weight: 1,000,000) was purchased from Sigma-Aldrich. Gelatin (from porcine skin, Type A, 300 mw) was purchased from Sigma-Aldrich. Matrigel was purchased from Corning (USA). Cellulose-based fibrous membranes were purchased from Filtros Anoia (FilterLab™, Barcelona, Spain).

2.2. Fabrication of spongy-like scaffolds

LAGG was dissolved in a beaker at 90 °C for 30 min in distilled water at 1 % (w/v). Gelatin was then added at 1% (w/v) at 60 ºC to make a total 2% (w/v) polymeric solution, under stirring. After homogeneous dissolution for 2 h, 1600 µL was added into a mold of 20x8 mm at 60 ºC. Afterwards, hydrogels were obtained by immersing the mold in Ca^{2+} at 0.25 M for 24h for total ionic-crosslinking of the LAGG molecular chains (gelatin was kept physically crosslinked). The formed hydrogels were frozen at -80 ºC and then freeze-dried. After 4 days, cylinders of 6x7 mm for *in vitro* trials were punched from the obtained dried structures. The structures were submitted to an ethylene oxide plasma treatment for sterilization before *in vitro* experimentation.

2.3. Dual-chambers design and fabrication

The dual-chamber bioreactor was designed to integrate two compartments interconnected by a central hole where a scaffold or membrane or 3D structure can be placed. A basket can also be inserted for hydrogel injection. The dual-chambers were fabricated in acrylic to be transparent, robust, and autoclavable. Medical-grade silicon O-rings were used to seal all the interfaces of assembling pieces. The design of the dual-chamber is provided in Figure S1. The bioreactor can incorporate twelve culture dual-chambers. The design of the dual culture chambers was conceived to avoid the total mixture of the culture media perfused in both compartments. In the bottom part of the culture dual-chamber was added a magnetic

Accepted Manuscript

bar to be attracted with the stirring position in the rotational platform described below. The sizes of each compartment were designed to fit a standard 6-well tissue culture plate.

2.4. Rotational platform design and components

A rotational platform designed to create a dynamic cell culture device to which the dual-chamber bioreactors can be magnetically attached. The platform was made of PLA and the backbone 3D printed (SAR, Portugal). Inside, a robotic system was assembled to coordinate the rotational movements in horizontal and vertical directions. A servomotor controller board was coordinating the mechanical rotations of 12 servos commanding the dual-chamber, and a 13th servo which was responsible for the vertical turning, both in 180º. The controller board was programmed so the horizontal rotational movement provided 15 different moving speeds for the rotational chambers. The vertical movement had configurable speed and turning was activated by a timer that could be set in seconds, minutes, and/or hours. The controller board provided Bluetooth® interface so an external device interacted with the system. Interfacing software for remote control of the device was developed for Microsoft (Figure S3) and Android (Figure S4) systems. Using the interface, the user could simultaneously configure the rotation speeds and timings for the system, while acquiring feedback on the temperature of each motor and remaining time for vertical rotation.

The horizontal rotation with two or more different programmable speeds, ranging from zero to 0.12 sec/degrees at no load, could be applied independently for each dual-chamber, which could be used as a mechanical stimulus for the cells cultured into a construct placed in that chamber. The vertical turning movement with a programmable time-delay was applied for all the dual-chambers to avoid cell sedimentation and control cell spatial distribution.

In any of the 12 positions could be magnetically attached a dual-chamber for cell culture. The dual-chambers could rotate until 180º (horizontal), being the rotations per minute controlled independently per position. The rotation was promoted by magnetic stirring, having magnets performing the attraction between the bottom part of the dual-chamber and the stirring position in the platform. The system was coordinated by an arduino (Atmel®) synchronized with a servo control module. The stirrer plate incorporated a wi-fi system to control the stirring at distance, using computer software. All the system could be placed inside a CO_2 incubator. This system was developed in collaboration with SAR - Soluções de Automação e Robótica, Lda (Portugal).

Accepted Manuscript

2.5. Micro-computed X-ray tomographic analysis

Micro-computed tomography (micro-CT) was used as a non-destructive imaging technique to scan scaffolds, which provided high resolution 3D images, resultant from the digital projection of 2D trans-axial images processed from the attenuation of X-rays passing through the sample's material. The obtained data set was processed by a set of software procedures. The microstructure and architecture of the fabricated structures were assessed using dry samples scanned by a high-resolution micro-CT (SkyScan 1272, Bruker, USA). 3D projections of the specimens were performed, with a pixel size ranging from 9 to 18 μm. Approximately 400 to 550 projections were acquired over a rotation angle of 180º or 360º, with a rotation step of 0.45º or 0.68º. Data sets were reconstructed using a standardized cone-beam reconstruction software (NRecon 1.6.10.2, Bruker). The output format for each sample was bitmap images. Representative data set of the slices was segmented into binary images with a dynamic threshold of approximately 30–255 for soft polymeric phase analysis (grey scale values – optimized per sample and analysis). Adjusts to these thresholds were performed according to samples formulation and materials sensitivity to X-rays. Then, the binary images were used for morphometric analysis (CT Analyser, v1.15.4.0, Bruker) and to build the 3D models (CTvox, v 3.0.0, Bruker). When needed, samples were vertically oriented in DataViewer (v1.5.2.3, Bruker) before proceeding to CT Analyser and CTvox.

2.6. Mathematical modelling and numerical simulations

2.6.1 Culture medium governing equations

In this process, culture medium is considered a continuity fluid. The incompressible medium movement is described by continuity equation (1) and Navier-Stokes equation (2) which are shown below:

$$\nabla \cdot \vec{\boldsymbol{u}} = 0 \qquad \textit{Equation 1}$$

$$\boldsymbol{\rho}\left(\frac{\partial \boldsymbol{u}}{\partial \boldsymbol{t}} + \boldsymbol{u} \cdot \nabla \boldsymbol{u}\right) = -\nabla \boldsymbol{p} + \boldsymbol{p}\vec{\boldsymbol{g}} + \boldsymbol{\mu}\nabla^2 \boldsymbol{u} \qquad \textit{Equation 2}$$

Where $\boldsymbol{u}$ is the culture medium velocity, $\boldsymbol{\rho}$ is the culture medium density. $\boldsymbol{p}$ represents pressure and $\boldsymbol{t}$ represents time. The filling process of culture medium is calculated by

Accepted Manuscript

volume of fluid (VOF) model which is aiming for simulate immiscible fluids having obvious interface—air and culture medium.

2.6.2 Cell dynamic seeding governing equations

Carried by culture medium movement, cells are represented as discrete particles, and its movement is simulated by discrete phase model (DPM). Cell trajectories are written in Lagrangian reference frame.

All cells are assumed as non-rotating during the whole simulation process. The equation of force balance on cell and the energy loss due to the inelastic collision has been described and validated in our previous work[16].

Furthermore, cell adhesion process is considered by four regimes, including stick, rebound, spread, and splash, which describe cell-material interaction when cells impinge a scaffold wall. In the stick regime, the cells that impact with the scaffold can remain in their original spherical shape. In the rebound regime, cells leave the wall intact but with different velocities. In the spread regime, cells hit the wall and spread out to form a wall film. In the splash regime, parts of the cell attach to the wall and other parts leave the wall. The impinge regimes, including stick, rebound, spread, and splash, are defined by the following equation (3):

$$\boldsymbol{E}^2 = \frac{\boldsymbol{\rho V_{pn}^2 d_p}}{\boldsymbol{\sigma}}\left(\frac{1}{\boldsymbol{min}\left(\frac{\boldsymbol{h_o}}{\boldsymbol{d_p}},1\right)+\frac{\boldsymbol{\delta_{bl}}}{\boldsymbol{d_p}}}\right) \qquad \textit{Equation3}$$

In this equation, E is a dimensionless value represent impact energy, $\boldsymbol{V_{pn}}$ is cell's velocity before impinging the wall of scaffold, $\boldsymbol{d_p}$ is the diameter of each cell, $\boldsymbol{\sigma}$ is the surface tension of culture medium, $\boldsymbol{h_o}$ is the film height of cells when they attached on the scaffold and $\boldsymbol{\delta_{bl}}$ represents the boundary layer thickness. The sticking regime occurs when the impact energy value is less than 16 and splash regime occurs when value is above 57.7.

In this simulation, spread and stick regimes are all for cells attached on the scaffold. The boundary layer thickness and critical transition temperature are defined by equations 4 and 5, as follows:

$$\boldsymbol{\delta_{bl}} = \frac{\boldsymbol{d_p}}{\sqrt{\boldsymbol{Re}}} \qquad \textit{Equation 4}$$

Accepted Manuscript

$$T_c = T_c^* \cdot T_s \quad \textit{Equation 5}$$

Where, Re is the Reynolds number. T_c^* represent critical temperature factor and set as 1 in this equation, which means that the saturate temperature T_s is equal to the critical transition temperature T_c.

2.6.3 Boundary conditions for cell seeding using one culture medium:

In this chamber, there are four pipes and two of them are on the top and other two on the bottom (see Figure 1, below). 1 bottom and 1 top pipe are set as inlets, from where the nutrient solution with cells is injected at 1 mm/s velocity. This speed was chosen because it is within the velocity of red cells in brain capillaries (0.3 to 3.2 mm/s)[17]. 50,000 cells are injected into the chamber, and they are assumed as 25 μm diameter spherical shape with 1.0×10^3 kg/m^3 density, 0.005 Pa·s for the viscosity and 0.03 N/s for the surface tension, based on our previous works[18,19].

2.6.4 Two type of nutrient mixing governing equations:

For dual chamber mixing process, two type of culture media (both water-based solutions of similar fluidic characteristics) are assumed as having water density aiming for cell culture to form interfaced tissues co-differentiation into two different type cells, or to keep heterotypic cultures. The conservation equation (6) of the liquids is described as follows:

$$\frac{\partial}{\partial t}(\rho Y_i) + \nabla \cdot (\rho \vec{v} Y_i) = -\nabla \vec{J}_i + R_i \quad \textit{Equation 6}$$

This convection-diffusion conservation equation of species transport is used to calculate the local mass fraction of each species and Y_i represents the two culture media. As this simulation solver is pressure based, R_i, the rate of culture media A and B at inlets consists of both convection and diffusion components. $\vec{J}_i$ represents the diffusion flux of culture media A and B due to their concentration gradients. Fick's law is used to calculate the diffusion flux, which could be written as in equation 7:

$$\vec{J}_i = -\rho D_{i,m} \nabla Y_i \quad \textit{Equation 7}$$

Where $D_{i,m}$ is defined as mass diffusion coefficient for nutrients in the mixture.

2.6.5 Two type of nutrient mixing boundary conditions:

Accepted Manuscript

In this process, 1 bottom and 1 top pipe are set as inlets with 2 different culture media, both water-based with the same density 1.0×10^3 kg/m^3 and velocity 1 mm/s. The other 2 pipes are set as closed pipe which means that no fluid would flow out from the system and there would be no more fluid injected into the system when the chamber is filled. After fulfilling the chamber, the injection is stopped, and the longitudinal or lateral rotation occur at 1rad/s. Please see Table 1, which compiles the boundary conditions.

Table 1. Boundary conditions for cell seeding and nutrient solution mixing

	Cell seeding	Nutrient solution mixing
Medium density (kg/m^3)	1.0×10^3	A & B:1.0×10^3
Velocity (mm/s)	1	1
Viscosity (Pa•s)	Cell: 0.005 Nutrient solution: 0.001	A & B: 0.001
Cell surface tension (N/s)	0.03	–
Cells density (kg/m^3)	1.0×10^3	–
Inlet speed (mm/s)	1	–
Rotation speed (rad/s)	–	1

The chamber and scaffold mesh are shown below (Figure 1). The scaffold is a cylinder with 6 mm height and 7 mm diameter.

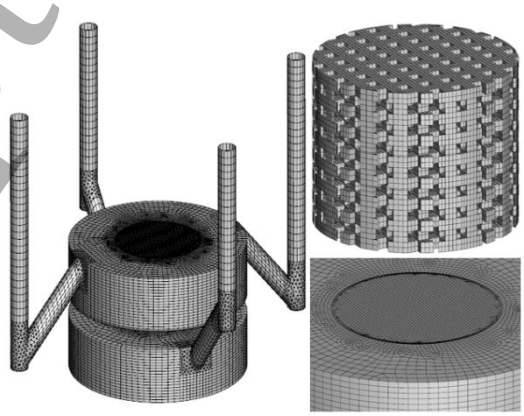

Accepted Manuscript

Figure 1. Chamber and scaffold mesh used for the computational simulations (total 182450 elements).

In the whole system, the scaffold is mainly composed of hexahedral meshes. The bioreactor without injection pipes is composed of hex- and tetra-meshes, and the middle part is also fully composed of meshes because cells attachment also occurs in the core of the scaffold. The pipe is mainly composed of hex-meshes and the connection area has high density of tetra-meshes to avoid cells entrapped in the corner if the bioreactor.

Software Fluent® (Ansys, Inc. v19.0, USA) was used to calculate all the conditions for the mathematical model. Additional computational simulations were also carried out using SOLIDWORKS® CAD software for broader particle and fluid behaviour analysis.

2.7. Isolation and culture of fat pad adipose-derived stem cells

Fat pad-ASCs were isolated from human tissues obtained from Hoffa's body removed during arthroscopic surgeries on male and female donors with ages between 19 and 32 years, after informed consent, under cooperation protocols established with Centro Hospitalar Póvoa do Varzim and Clínica Saúde-Atlântica. The protocol was ratified by the Ethical Committee of Centro Hospitalar Póvoa do Varzim, Grupo Saúde-Atlântica and University of Minho.

All the samples were handled within 24 h after the arthroscopic procedure to the knee. Human ASCs (hASCs) were isolated following an enzymatic digestion-based method with type II collagenase (Sigma). The extracted tissue was placed in PBS solution and washed several times with PBS containing 1 % (v/v) antibiotic (AB) mixture, until total removal of blood and cut into small pieces. Tissue digestion was performed by incubation at 37°C in a humidified atmosphere of 5 % CO^2 for 10 h in a 10-20 mL 1:1 mixture of Minimum Essential Media alpha (MEM alpha, Invitrogen) supplemented with 10 % fetal bovine serum (FBS, Gibco) and 1 % AB mixture, with type II collagenase 0.15 % (w/v) in PBS. The digested tissue was filtered and cell suspension centrifuged at 300 g for 5 min. The hASCs were selected by plastic adherence and expanded in α-MEM medium supplemented with 10 % FBS and 1 % of AB mixture.

2.8. Other cell types and culture

Accepted Manuscript

hCoMECS (Innoprot, Spain) were routinely cultured under the conditions defined by the supplier company over a coating of gelatin type A (0.7 % w/v). Tissue culture plates was covered with gelatin solution (0.2 % w/v) for 30 min at 37 ºC before washing with PBS. Cells were cultured with EndoGRO-MV Complete Media Kit (Millipore, USA) and routinely trypsinized for 5 min at 37 ºC in TryplETM Express (Life Technologies, UK), centrifuged (220 g, 5 min) and re-suspended at a cell density of 10^3 cells/cm^2 in T150 flasks.

SH-SY5Y neuroblastoma cells were plated at 1×10^6 cells/cm^2 on 10 µg/ml laminin, cultured in Dulbecco's Modified Eagle Medium/Nutrient mixture F-12 (DMEM/F-12, Thermo-Fisher Scientific), containing 3% FBS (Thermo-Fisher Scientific) and 1% penicillin-streptomycin (Life Technologies). SH-SY5Y human cell line was expanded keeping both the adherent and floating cells, which correspond to epithelial- and neuroblast-like cells, respectively[20]. Both adherent and floating cells were expanded and collected when cells were passed. Floating cells were removed in culture medium, whereas adherent cells were detached with trypsin. The two cell populations were combined, centrifuged, and re-plated until the required cell number for the study was obtained. Both cells were also encapsulated in the hydrogel used for the model. SH-SY5Y floating cells were *in situ* (dual-chamber) differentiated to a more mature neuron-like phenotype that is characterized by neuronal markers, as described in section 2.14.

2.9. Live-dead assay performed in the prototyped scaffold and in the LAGG-gelatin sponge

Calcein-AM and Ethidium Homodimer-1 (EH) - live-dead assay - was perform at day 3 to observe the distribution of live and dead cells in each condition (static vs vertically rotational culture). 1M cells were cultured per scaffold. A vertical rotation was performed every 30 min during the first 6 h. The distribution of cells in the scaffold was compared to the control (static chamber). Cell viability within freeze-dried structures was assessed by staining cells with calcein-AM (1 µg/mL, Invitrogen, USA) for 1-2 h and EH (2 µg/mL, Invitrogen, USA) for 20-30 min at 37 ºC in a humidified tissue culture incubator with 5 % CO2 atmosphere. The green staining was quantified in a color histogram per condition and per region (top, middle and bottom) using Fiji®.

2.10. Rotational movement performed in the GG-gelatin sponge

Accepted Manuscript

After cell seeding at 1M cells per scaffold, 1600 µL of α-MEM was added to the static control for each construct supplemented with 10 % FBS (Thermo-Fisher Scientific), 1 % penicillin-streptomycin (Life Technologies). The same culture medium was used as described before, being perfused at 1rad/s (10 rpm) speed in the dynamic rotational conditions.

2.11. Alamar blue® assay for metabolic activity quantification

In vitro metabolic activity was assessed at day 3 of culture using AlamarBlue® CellTiter-Glo Luminescent Cell Viability Assay (Promega, Madison, WI, USA) (n = 9), at 37°C in a humidified 5 % CO_2, in a dilution of 10 % in culture medium. Then, the medium was removed by aspiration and the constructs were washed with fresh medium three times and kept in culture until the end of the assay. The reacted AlamarBlue® was read in a microplate reader (Synergy HT; BioTek, VT, USA) at 570 and 600 nm, respectively. And then, the reduction percentage of AlamarBlue® was calculated following the protocol from the manufacturer.

To assess the metabolic activity obtained using the dual-chamber bioreactor under horizontal rotations compared to a static culture condition (control), a GG-Gelatin 1:1 (w/w) scaffold (monolayer) was used to culture hASCs from fat pad. Metabolic activity of cells cultured in dual-chambers under horizontal rotation at 1 rad/s (10 rpm) *versus* static was measured. An increase of metabolic activity was observed at day 3 of cell culture. Scaffolds without cells were used as a negative control for fluorescent intensity correction.

2.12. mRNA quantification

Total mRNA was extracted from cells cultured per condition at day 3 using RIBOZOL™ RNA extraction reagent (VWRCN580, VWR). Nanodrop 1000 (ThermoScientific, USA) was used for the quantification.

2.13. Dual-flow in dual-chambers performed with food dyes

Food dyes were used to assess the creation of horizontal and vertical colour diffusional gradients when perfused through the dual-chamber bioreactor at 3 µL/min, controlled by a syringe pump (New Era Pump Systems, USA) with 10 mL syringes (Braun, Germany). This flow rate was chosen based on the native blood-brain-barrier average permeability rate for

Accepted Manuscript

small molecules [21]. Images were captured with a continuously recording camera (Cannon, Japan). Fiji® was used to slice the captured bioreactor vessel into three similar regions and perform the RGB histogram quantification.

2.14. Blood-brain-barrier model

Pre-conditioned hASCs with 1 ng/mL TGF-β1 (ebiosciences, USA) over 7 days (CD146-positive cells), were induced as previously reported by our Group[22], were co-cultured with hCoMECs. Cellulose membranes in the dual-chamber were directly seeded with hCoMECs (1M cells single culture), or pre-seeded with hASCs 3 hours before a seeding with hCoMECs (1M cells co-culture 1:4 ratio, respectively), keeping a total number of 1M cells in both conditions.

SH-SY5Y were embedded in Matrigel® (3M cells per 100 µL) and cultured over 7 days in the opposite compartment of the dual-chamber. SH-SY5Y were cultured with DMEM-F12 and 5% FBS (Thermo-Fisher Scientific), 1% penicillin-streptomycin (Life Technologies), and supplemented with 10 µM all-trans retinoic acid (RA; Sigma Aldrich), while the endothelial condition was cultured in EndoGRO-MV complete kit, at 37 °C, in a humidified atmosphere with 5 % of CO_2, which constituted both culture media perfusing the dual-chambers.

Molecular permeability test was conducted to assess the living membrane permeability in alternative to the traditional trans-endothelial electrical resistance (TEER) test, since the second was not available in the laboratory. To do so, fluorescent-dextran 70 kDa (15 µg/mL, Sigma Aldrich), a marker that do not cross the human BBB[23], was perfused in the top compartment and its fluorescence quantified from the media collected from the top and bottom compartments.

2.15. Flow Cytometry

Flow cytometry was performed using mouse anti-human antibodies CD146 (unconjugated, abcam, UK), CD73 (PEconjugated, BD biosciences, USA), CD90 (APC-conjugated, ebiosciences, USA) and CD105 (FITC-conjugated, AbD Serotec, UK). Human Hoffa's Body-derived ASCs, perivascular-like (CD146+) cells were trypsinized, counted and resuspended in a 2% BSA (Sigma, Canada) solution in PBS (BSA/PBS) at a concentration of 10000 cells/mL. Cells were first incubated for 45 min at 4 ºC, protected from light, with CD146

Accepted Manuscript

antibody (1:100). After a washing step with PBS, cells were incubated for 45 minutes, protected from light, at room temperature with AF488 conjugated secondary antibody (goat anti-mouse, Molecular probes, USA) at a concentration 1:500. After a washing step, cells were resuspended in PBS and at least 1000 events were analysed using a FACSCalibur flow cytometer (BD Biosciences) and the CELLQuest software V3.3.

2.16. Immunocytochemistry

hASCs (green) and hCoMECs (red) were live stained using CellTracker™ Green CMFDA Dye and CellTracker™ CM-DiI Dye (Thermo-Fisher), respectively, following supplier instructions. After cell culture within hydrogels or freeze-dried structures, the constructs were first fixed with 10 % v/v of formalin (Thermo Scientific, USA) for 30 min and then cell-laden materials were cut into thin slices or observed under fluorescent microscope if translucent constructs were obtained after staining. Cells were permeabilized with 0.1 % v/v of cold Triton-X 100 (Sigma) for 30 min and blocked with 3 % w/v of bovine serum albumin (BSA, Sigma-Aldrich) for 60 min. Neuron's microtubules biomarker from central and peripheral nervous system, Anti-TuJ1 (class III β-tubulin, abcam, ab18207) host rabbit, anti-mouse, was used at dilution 1:200 in 1 % (w/v) BSA/PBS for 24 h at 4 ºC. Later, cells were washed three times with PBS and incubated with secondary antibodies Alexa Fluor 488 overnight at 4 ºC, and according to the host of the primary antibody. Finally, cells were again washed in PBS and counterstained with DAPI (0.02 mg/mL; Invitrogen, USA) for 15 min for nuclei counter-staining. Cells were observed using an AxioImager Z1m fluorescence microscope (Zeiss, Germany), a LSM710 inverted confocal microscope (Zeiss, Germany), or with a TCS SP8 confocal microscope (Leica, Germany).

2.18. Computed microscopic analysis by Fiji®

Fiji® is an image processing package distributed by ImageJ, bundling plugins for scientific image analysis. Fiji® was used to quantitatively evaluate the mixing dyes from the RGB histograms of red and blue phases, over time, and at the bottom, interface and top regions of the dual-chamber. When necessary, Fiji® was also used to quantify the outcomes from immunocytochemistry.

Accepted Manuscript

2.19. Statistical analysis

Statistical tools were employed to identify whether statistical differences existed between the parameters measured. GraphPad (GraphPad Software Inc., USA) and Microsoft Office Excel (Microsoft, USA) were used to perform statistical analysis. Results were shown as mean ± standard deviation (SD) or confidence interval (CI) of at least triplicates and then averaged. Biological results were performed at least in three independent experiments (n=3). SD and CI are reported as measure of sample deviation. When more than two groups and/or treatments were compared at the same time, one-way ANOVA test was applied using Tukey-Kramer method as a post-hoc pairwise comparison test. A p-value < 0.05 was considered statistically significant.

Accepted Manuscript

3. Results

3.1. Manufacturing and development of dual-chamber bioreactors and dynamic platform

A dual-chamber bioreactor was designed and developed. The dual-chamber is composed by two inlets and two outlets, a top cap, a middle component which accommodates the cell culture environment, and a bottom cap, where a magnet can be placed allowing a magnetic attachment to the dynamic platform (Figure 2A).

The dual-chamber bioreactor is miniaturized, with a central hole where a custom-made holder, basket, scaffold, or membrane can be placed, and fully transparent to facilitate cell culture monitoring and imaging (See supplementary videos 1 and 2).

A dynamic platform was conceived, with twelve magnetic positions governed by twelve servo motors (Figure 2B). The platform exoskeleton was 3D printed, where the dual-chamber bioreactors are attached to the twelve servo motors, programmed and controlled through a Bluetooth® system (smartphone application or computer software, Figures S2 and S3). Each position is monitored for servo temperature and its rotation speed controlled in real-time by the application. The dual-chambers were designed to fit standard 6-well culture plates, serving as a versatile alternative or static control condition (Figure 2C).

Accepted Manuscript

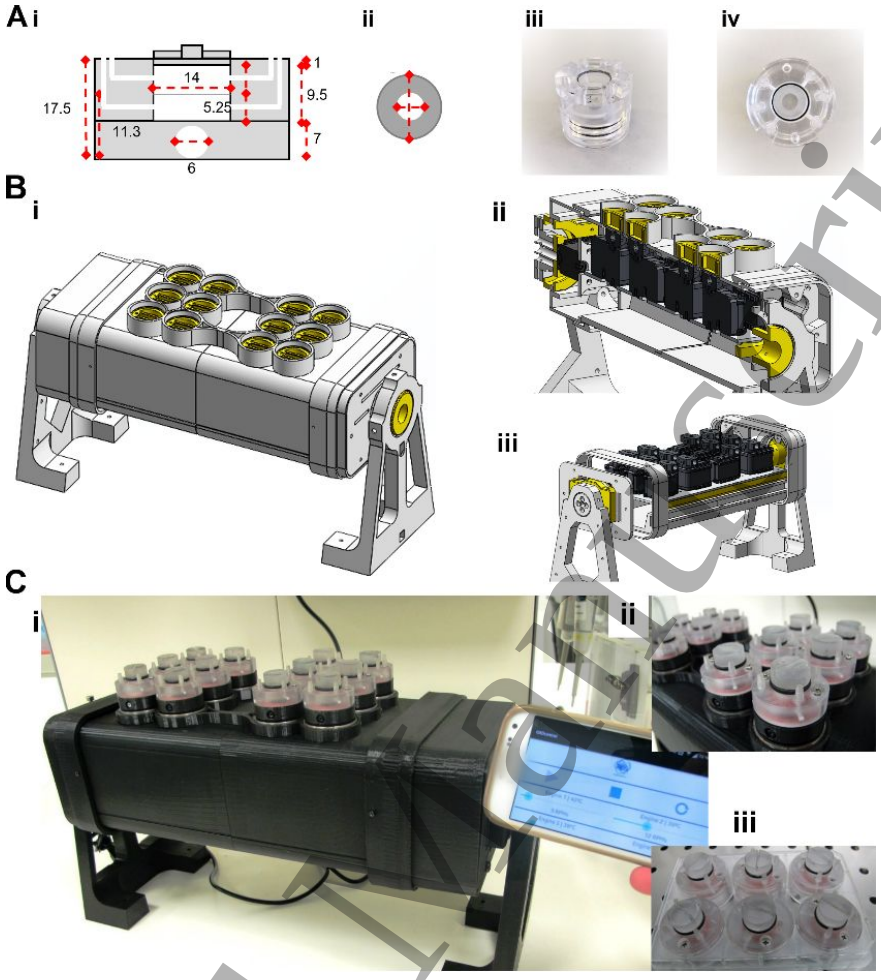

Figure 2. Designed dual-chamber bioreactor and dynamic platform. (A) A dual-chamber bioreactor was designed to accommodate two inlets and two outlets feeding two interconnected compartments. The dual-chamber (i) cross-section and (ii) central barrier were represented to show each component size (millimetres). (iii) A perspective and (iv) top view were photographically captured showing the chamber transparency. (B) The dynamic platform to induce vertical and horizontal rotations was designed. (i) Perspective, (ii) lateral and (iii) top cross-sections were depicted. (C) The final assembled bioreactor system was prototyped. (i) The 3D printed platform with attached dual-chambers was pictured along with the smartphone with the application controlling the platform through Bluetooth® connection. (ii) A closer view of the dual-chamber on the platform was represented, as well as (iii) the dual-chamber in a standard 6-well culture plate.

Accepted Manuscript

3.2. Computational simulation and experimental assessment of cell seeding and distribution in dual-chambers

The fluidic injection on top and bottom inlets was computationally simulated and the speed per millimetre relative to the chamber position tracked. A peak entering each compartment from the inlets, followed by a decrease down in the larger volume of each compartment was observed. A maximum of 2 mm/s was registered at the inlet, reaching then a steady state inside the larger culture environment that ranges from zero to 0.15 mm/s (Figure 3A).

Furthermore, a simulation was run for the cell seeding. In this case, spherical particles with an average 25 μm diameter were designed and computationally injected in the dual-chamber bioreactor (Figure 3B-i). Using environmental pressure as boundary condition, a maximum and lower pressure of 101200 and 101000 Pa were registered, respectively. A maximum speed of 0.836 mm/s was computed using an initial injection speed of 0.4 mm/s. The simulated cells were projected to the top of a prototyped simulated scaffold, crossing the full length of the structure and reaching the bottom surface of the culture chamber. Importantly, in this computational modulation, no adhesion properties were considered (Figure 3B-ii).

Additionally, the simulated cells were injected on the top and bottom inlet and cells' accumulation in the scaffold region was calculated over 360 seconds. The accumulated cell mass, in kilograms, varied from $3.28e^{-22}$ Kg at 240 seconds to $2.26e^{-21}$ Kg at 360 seconds, showing the ability to perform cell seeding in the central scaffold using the chamber inlets (Figure 3C).

Accepted Manuscript

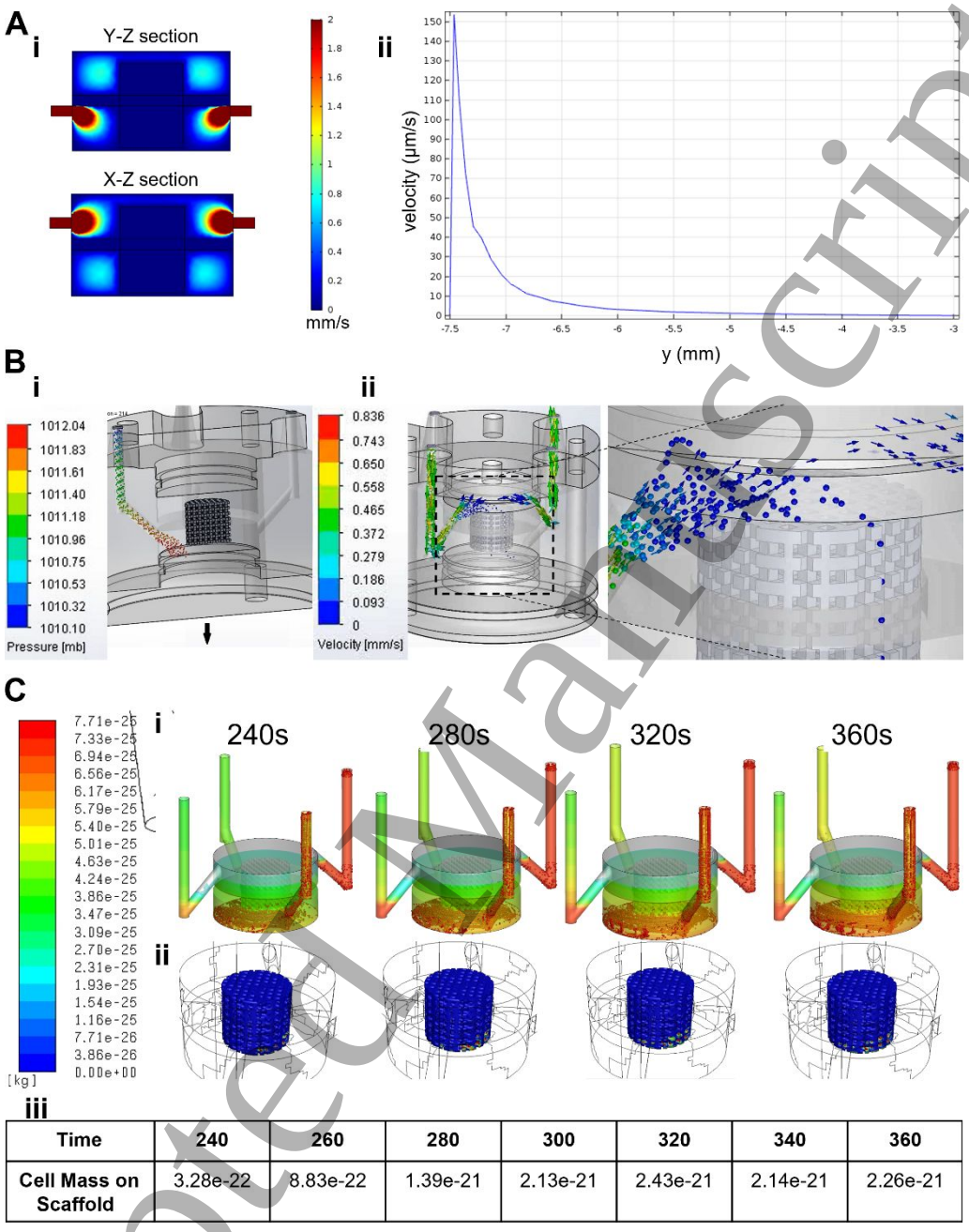

Time	240	260	280	300	320	340	360
Cell Mass on Scaffold	3.28e-22	8.83e-22	1.39e-21	2.13e-21	2.43e-21	2.14e-21	2.26e-21

Figure 3. Cell seeding into the dual-chamber bioreactor. (A) The inflow of water-based culture medium was simulated in the top and bottom compartments and the perfusion speed was calculated (Fluent®). (B) The cell seeding was simulated by a computed injection of spherical elements of 25 µm diameter (SOLIDWORKS®). (i) A first representation shows the injection of the micro-particles in the bottom compartment, having the gravity force pointing down. (ii) A second representation shows the same microparticles injected in the bottom compartment, and the image is magnified to provide a better visualization of the simulation. (C) The injection is simulated and represented overtime, (i) represented in images up to

Accepted Manuscript

360s. (ii) The presence of particles inside the prototyped scaffold (blue) is represented in red, (iii) and the total cell mass, which is represented by particles mass in the simulation, is demonstrated for the specific period (Fluent®).

NIH/3T3 cells were seeded onto the prototyped scaffold using the top and bottom inlets of the dual-chambers. After three days of cell culture, the top, middle, and bottom regions of the construct were assessed (Figure 4-i), using fluorescence microscopy to capture a live-dead assay. A homogenous cell distribution and viability was revealed (Figure 4-ii and 4-iii). Moreover, no significant differences were observed between evaluated regions, demonstrating, once more, a consistent cell distribution within the prototyped scaffolds (Figure 4-iv).

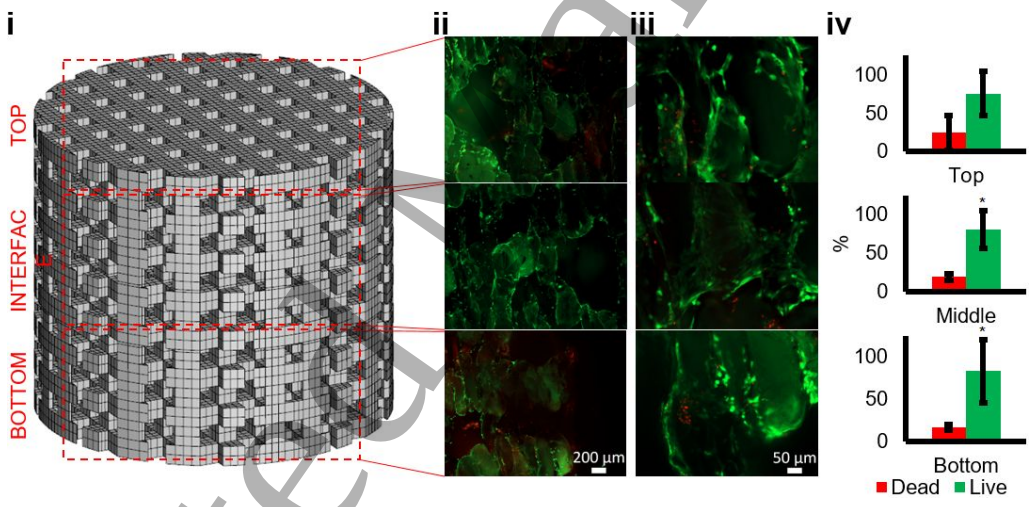

Figure 4. Cell viability after seeding into the dual-chamber bioreactor. (i) Prototyped PCL scaffolds were 3D printed to support cell adhesion using the same architecture of the simulated scaffold. NIH/3T3 were seeded through the inlet and outlet of the dual-chamber bioreactors and cultured over 3 days. (ii) Low, and (iii) high microscopic magnifications were used to assess the performed live-dead assay. Green colour corresponds to calcein staining for live cells, red is ethidium homodimer-1 for dead cells. (iv) Live-dead immunostaining was quantified per region (N=6). Data expressed as Mean ± Confidence Interval (*p value < 0.05).

Accepted Manuscript

3.3. Computational simulation and experimental assessment of vertical rotation after cell seeding

After having tested mouse fibroblasts in prototyped scaffolds, human stem cells were cultured in a spongy-like hydrogel to assess the viability and distribution of adherent cells under vertical rotation, since it represents a more biomimetic construct compared to the prototyped PCL (Figure 5B). Yet, the used spongy-like scaffolds presented an average pore diameter of 568 ± 97.2 μm, in the range of the 500 μm pore size of the prototyped PCL scaffolds previously simulated (Figure 3) and experimentally tested (Figure 4). This evolution from a prototyped structure to a spongy-like one in the developed work was intended to show the versatility of the dual-chamber bioreactor, and to corroborate the system for different scaffolds.

To assess the culture medium flow under the stimulation of a vertical rotation, using computer simulation, two rotation speeds were tested, such as 0.5 rad/s and 1 rad/s (Figure 5A-i and ii, respectively). At 1 rad/s, the rotated flow ranges from 0.3 to 1 rad/s, while at 0.5 rad/s, the flow is homogeneously rotated, confirming that there is a perfusion stimulus in scaffold with an average pore size of 500 μm when vertically turning the culture dual-chamber.

Having this into consideration, human adipose-derived stem cells (hASCs) were seeded at low cell density in a blended low acyl gellan gum-gelatin (LAGG-Gelatin 1:1) spongy-like hydrogel to assess the distribution of cells in the scaffold. A static condition was used as a control (no rotation). In Figure 5B-ii, it is possible to observe cell sedimentation in the static control, while higher density of cell adhesion is observed in the vertical rotational culture. This difference was quantified and represented in Figure 5B-iii. Strikingly, a significantly higher number of viable cells was observed on the top region of the scaffold compared with the static condition, which is a result of the vertically turning culture.

Accepted Manuscript

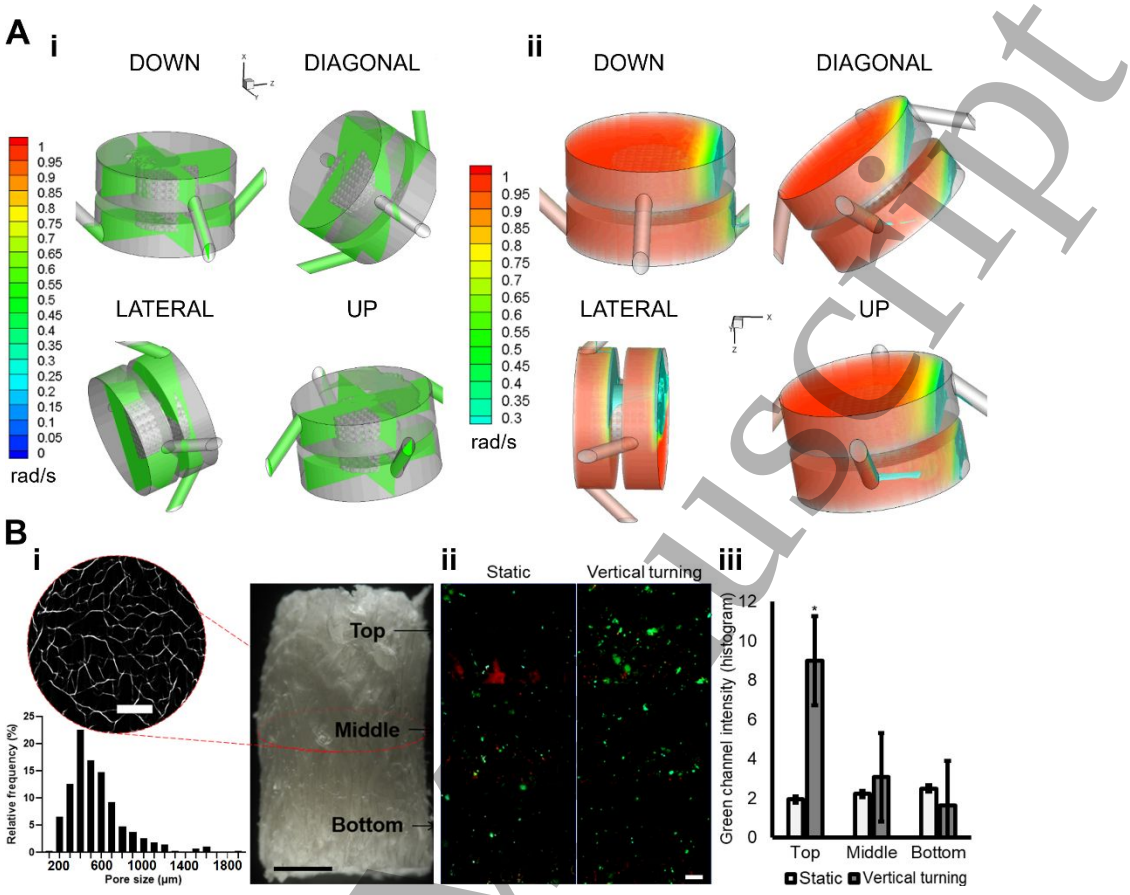

Figure 5. Vertical dual-chamber rotation. (A) A computational simulation was performed to assess the flow speed promoted by vertical rotation at two different rotations speeds (SOLIDWORKS®), (i) 0.5 rad/s, and (ii) 1 rad/s. The liquid motion was captured when the dual-chamber was turned down, diagonal, lateral, and up. (B) Human adipose-derived stem cells were cultured in a (i) low acyl gellan gum-gelatin (LAGG-Gelatin) spongy-like hydrogel with a cross-section demonstrating pore distribution. The top, middle, and bottom regions were assessed (scale bar = 3 mm). (ii) Cells were seeded at low density to assess their distribution in the three regions under static (control) and vertical turning stimuli. A live-dead staining using calceín (green) and ethidium homodimer (red) was performed at day 3 to assess cell viability and distribution (scale bar = 200 µm). (iii) The living and dead cells were quantified and graphically represented. Data shown as Mean ± SD (*p value < 0.05, N=3).

3.4. Biochemical gradient stability and media exchange in dual-chambers under horizontal rotation

Accepted Manuscript

Horizontal rotation was also studied using computational simulation, and the vectors of fluid trajectories were represented (Figure 6A-i). When the chamber is rotated at 0.5 rad/s, the fluid linear speed outside a prototyped scaffold reaches 32.516 mm/s, while the linear speed of the fluid in the inner portion of the chamber, through the scaffold porosity, ranged from 2 to 10 mm/s, if the fluid was flowing in the core or in the outer part of the scaffold, respectively.

To assess the effect of the performed rotational stimulus over cell metabolic activity and viability, the cultured hASCs were compared in static and rotational (horizontal) conditions (Figure 6B-i), demonstrating an increase in metabolic activity of 58.6% (Figure 6B-ii), and an enhancement of RNA transcription activity, while the static culture resulted in a significant decrease in this last indicator (Figure 6B-iii).

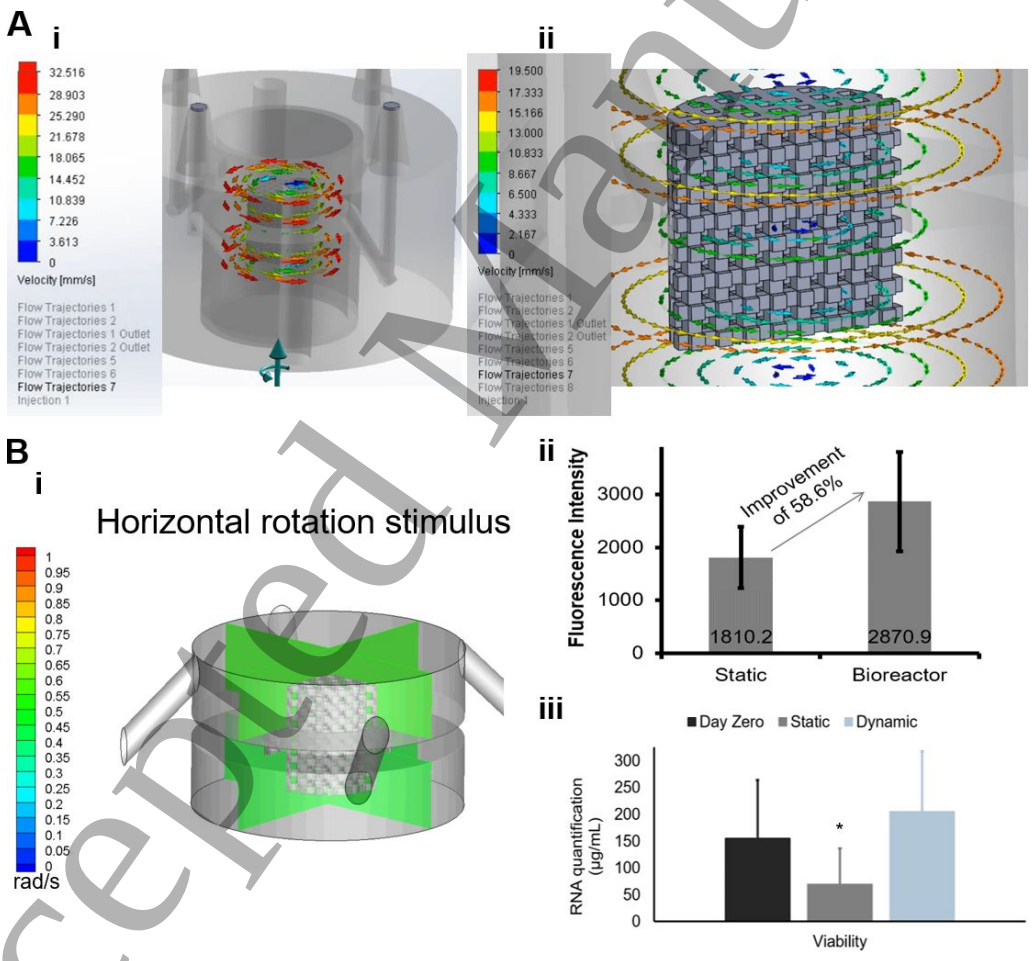

Figure 6. Horizontal dual-chamber rotation. (A) A computational simulation was performed to assess (i) the overall fluid speed in the chamber, as well as its speed (ii) inside a prototyped scaffold, used as a representative case-study (SOLIDWORKS®). (B-i) The fluid occupies the full chamber (Fluent®) and its effect over (ii) ASCs metabolic activity, and (iii)

Accepted Manuscript

genetic transcription activity was assessed at day 3. Data shown as Mean ± SD (p value < 0.05, N = 3).

To assess the effect of the inversion of gravity in the perfusion of two parallel flows of culture media, resulting from a vertical turning of the chamber, a computational simulation was evaluated (Figure 7A). The fluid injected at a flow rate of 0.05 mm/s reached a steady state when entering the chamber volume, ranging from zero to 0.009 mm/s, and its flow vectors were not considerably affected by the inversion of the gravity force vector.

Moreover, the perfusion of two different fluids was experimentally tested. Using food dyes, yellow and blue fluids perfused the top and bottom compartments of the dual-chamber, respectively (Figure 7B). In the top and bottom compartment, three subjacent regions along the X-axis were quantified (Figure 7B-i). A homogeneous mix of yellow and blue were observed in both compartments, having about 75% of yellow in the top, and 70% of blue in the bottom compartment, respectively. Similarly, three subjacent regions were quantified along the Z-axis (Figure 7B-ii), observing the formation of a gradient of yellow and blue fluids from the top to the bottom compartments, having about 75% of yellow in the first, 50% of each in the interface, and 75% of blue in the bottom compartment.

Results demonstrated in Figures 6 and 7 showed that it was possible to keep a perfused construct either under rotational conditions without connected tubing (Figure 6), or with connected tubing injecting culture media (Figure 7-B).

Accepted Manuscript

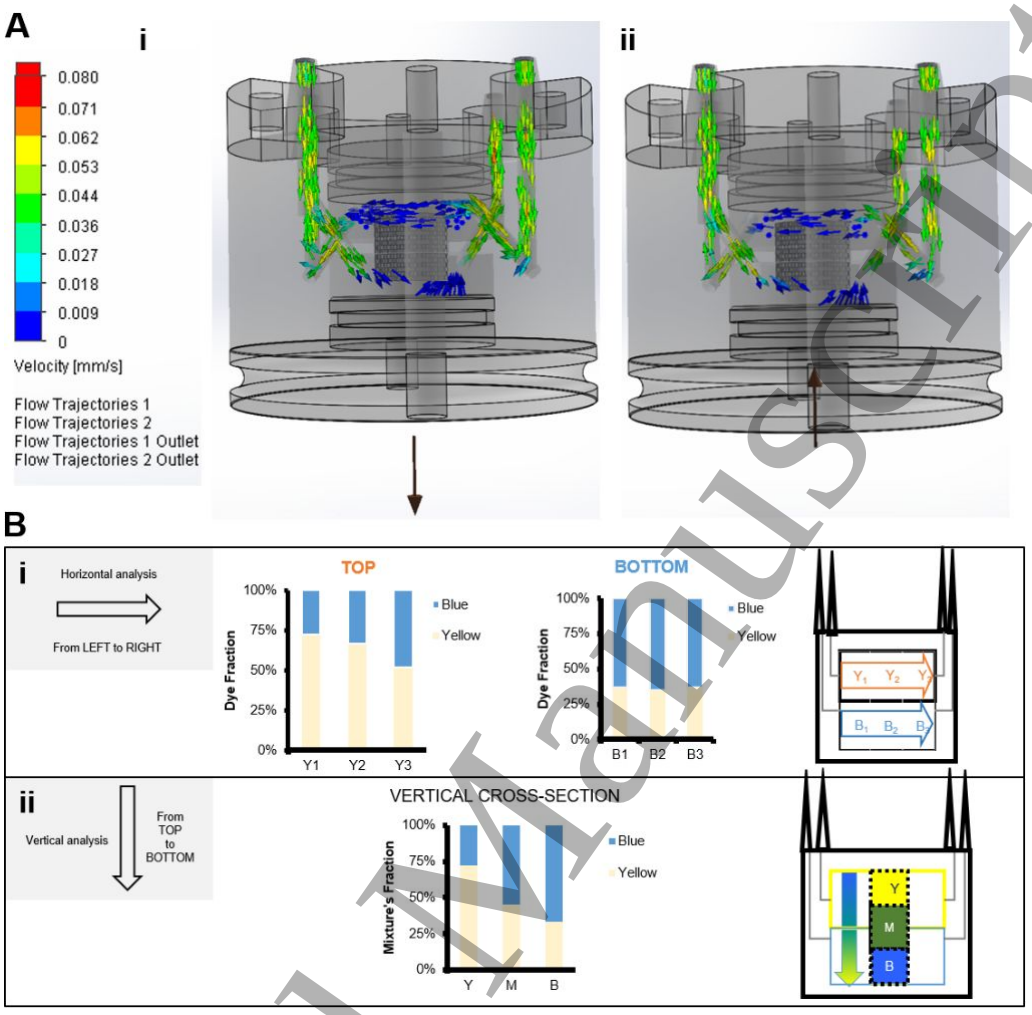

Figure 7. Fluid mechanics in multi-chamber system. (A) A computational simulation was performed to assess the influence of gravity (the arrow under the chamber represents its direction) on the fluid speed, (i) with gravity direction downwards and (ii) with gravity direction upwards, corresponding to the situation where the chamber is inverted compared to (i) (B) The amount of yellow and blue fluids was quantified per compartment in (i) three subjacent regions along the horizontal X axis. Controlled fluidics mix was obtained in both compartments of the dual-chamber, while a majority of the yellow fluid in the top, and blue fluid in the bottom, are maintained per compartment. (ii) The vertical mixing of the two fluids was assessed in the top, middle, and bottom regions of the chamber. A gradient mix was registered from the top to the bottom compartments, as graphically and schematically depicted.

Accepted Manuscript

3.4. Molecular permeability of a heterotypic blood-brain-barrier *in vitro* model under adjacent flow streams

Targeting a heterotypic tissue, composed by a complex endothelial barrier, both monoculture and co-culture of hASCs with Human Colonic Microvascular Endothelial Cells (hCoMEC) were performed to assess their permeability to Dextran 70 kDa. Also, SH-SY5Y (sub-line of the human neuroblastoma SK-N-SH line) were used to constitute the neural construct in the opposing compartment, with a multi-phenotypic cellular composition including epithelial and neural cells[20] (Figure 8A).

Accepted Manuscript

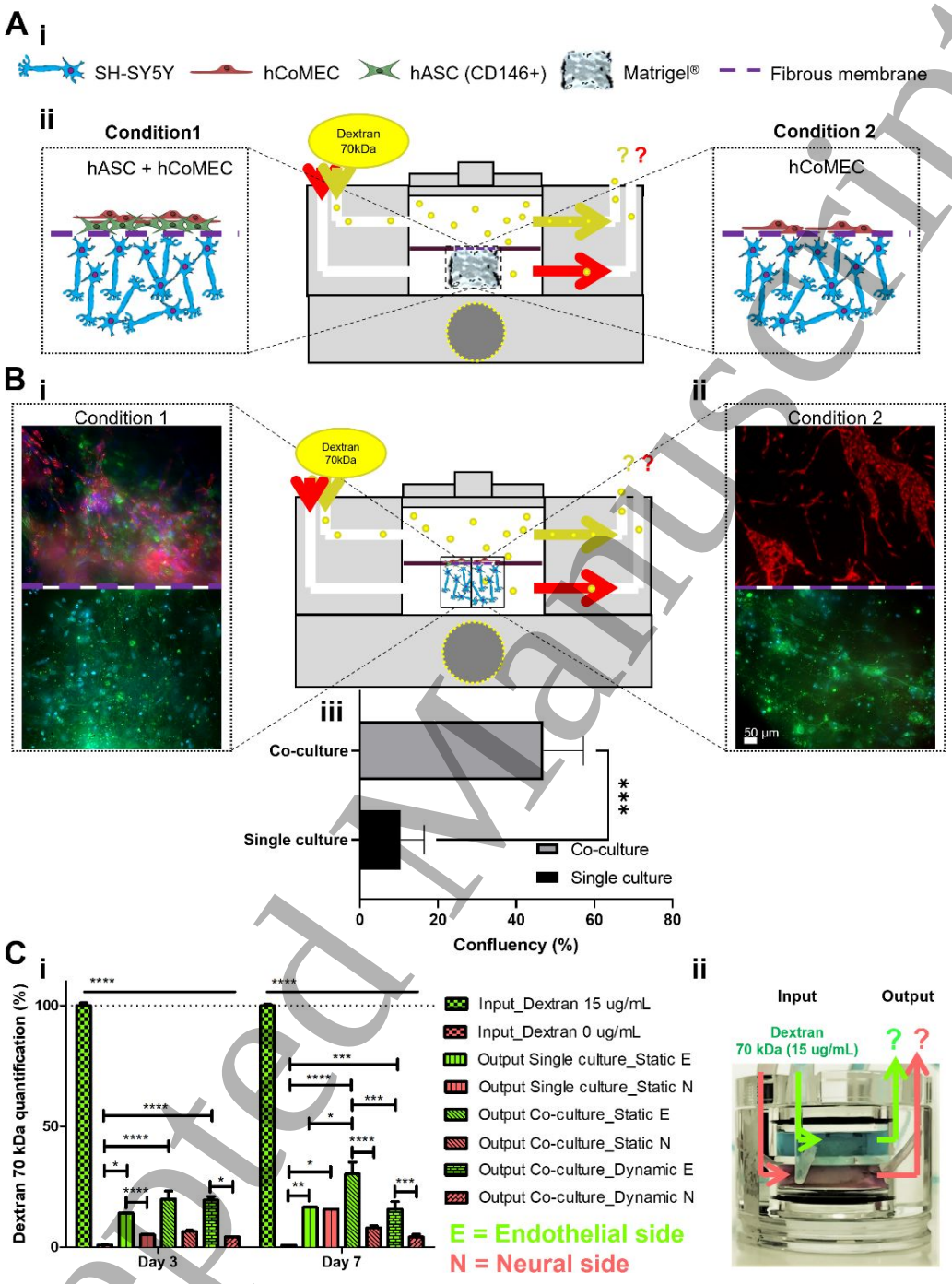

Figure 8. Molecular diffusion in a 3D BBB model. (A) A BBB model was mimicked using (i) SH-SY5Y as a neural and epithelial cell line model encapsulated in Matrigel®, while hCoMEC were used as endothelial cells. CD146+ hASCs were added as a co-culture to recapitulate the pericytes in the endothelial BBB. (ii) Endothelial layer composed by a co-culture of hASCs and hCoMECs was used as condition 1 and compared with condition 2, where an endothelial layer was composed by a single culture of hCoMECs (***p < 0.0001).

Accepted Manuscript

In both conditions, cellulose nanofibers were used as a support for cell adhesion. Dextran was injected as a standard marker for endothelial permeability since 70 kDa dextran is known to do not overcome the native human BBB. (B-i) The co-cultured layer of hCoMECs and CD146+ hASCs, (ii) as well as the single culture, were assessed. (iii) Cell confluency distribution was assessed using Fiji® [24] for each culture condition. The 3D heterotypic culture of epithelial and neural cells was kept on the bottom compartment. Live staining was performed for the hCoMEC (red) and hASCs (green). Immunostaining with TUJ1 (green) and DAPI (blue) was performed to assess the neural and nuclei arrangement in the bottom compartment, respectively. (C) Two different culture media were perfused, an endothelial and a neuronal, respectively, and the amount of Dextran nanoparticles was assessed per top and bottom outlet (*$p < 0.05$, ** $p < 0.01$, *** $p < 0.001$, ****$p < 0.0001$).

To build the model, two different conditions were engineered. Condition 1 was composed by pericytes-like CD146+ hASCs (Figure S6) co-cultured with hCoMECs on top of a cellulose matrix (fiber thickness = 21.5 ± 2.36 µm; pore size = 8.85 ± 1.73 µm; mean porosity = 28.8 ± 3.27 %; Figure S5), while Condition 2 was composed by a monoculture of hCoMECs. The same cell number was kept in both conditions. Moreover, SHSY5Y were kept under neurogenic culture conditions in Matrigel® in the bottom compartment (Figure 8B). This cell line is composed by two main phenotypes, epithelial and neuronal ones [20]. Cell confluency in the BBB-like membrane was significantly increased when CD146+ hASCs are co-culture with hCoMEC, while keeping the same total cell number in both conditions.

To assess the engineered tissue barrier permeability, perfusing fluorescent Dextran 70 kDa, the collected medium from the bioreactor system was evaluated through fluorescent spectroscopy. The presence of Dextran 70 kDa was quantified per compartment and condition, under static (single- and co-cultures) and dynamic co-culture. A significantly higher amount of Dextran was found crossing the barrier in the single culture condition compared with the co-culture one in both, static and dynamic condition. At day 7, the amount of dextran in the neural and endothelial compartments in the single culture condition reached an equilibrium, being similar in both compartments. This revealed a high permeability of the endothelial layer in single culture.

On the other hand, in both static and dynamic co-cultures, the membrane composed by endothelial and hASCs was able to keep higher amounts of Dextran in the endothelial side

Accepted Manuscript

compared with the neural compartment, over 7 days (Figure 8C). This quantification revealed an improved BBB-like membrane impermeability in the co-culture compared with the single culture. Particularly, when tested under dynamic conditions less Dextran was quantified. This was correlated with the interference of the rotational movements and the low perfusion when collecting the dye from the dynamic model, since in static cultures the collection was manually pipetted.

Accepted Manuscript

4. Discussion

Although TE bioreactors, and *in vitro* modelling platforms, have been viewed as potential alternatives to the conventional use of 2D cell culture systems and animal models, respectively, its effective translation to industrial and clinical practices is still limited. Likely responsible for the delayed translational process are poorly standardized outcomes, laborious systems, and lack of dynamics mimicking the *in vivo* scenario.

Starting from this paradigm, the bioreactor system described in this work represents a versatile and compact platform to effectively control cell seeding homogenization in 3D scaffolds, tune perfusion stimulation with connected tubing or even in a tubing-free set-up by means of using rotational (vertical and horizontal) stimulation of individual dual-chambers. The design and development of the system are scalable and user-friendly, enabling a wider use of the system by industry and researchers in the academic sector. The bioreactor system has already been sent to a number of research labs, running successful experiments with minimal training, while used in a variety of biological applications.

In this context, bioreactors are devices conceived to deliver proper spatial and temporal nutrient transport that may also induce mechanical or other physical stimulation, in a well-defined environment[7]. Bioreactors that provide controllable environments are suitable to act as units for large-scale tissue fabrication and bioprocesses[8]. Furthermore, bioreactor systems can also provide reliable, efficient tissue modelling platforms for fundamental studies of cell biology and drug testing [9]. Herein, the developed rotational platform exoskeleton was entirely 3D printed, facilitating a cost-effective production of the system. Also, fully transparent chambers were produced to enable the user to efficiently perform specific evaluations of interest (e.g. fluorescence analysis) and microscopic evaluations under visible light. Nevertheless, the device allows to continuously keep the system inside the incubator, using Bluetooth® connection with an external device (e.g. smartphone, tablet, or computer) to control the rotational speeds, monitor each motor temperature, and to start and stop the equipment.

Several bioreactors have been reported, including mixed flasks[10], rotating vessels[11], perfused cartridges[12], and bioreactors with mechanical stimulation[13]. Additionally, dual-chamber bioreactors and oscillating bioreactors have also been described for TE[25,26]. Other systems have been described as inventions in patents for automated cell culture[27], including detection sensors[28], specialized chambers to mature constructs for TE with

Accepted Manuscript

electrical or mechanical stimulation[29], or even oscillating cultures[30]. However, the main limitation of the disclosed bioreactors for TE is that the newly formed tissue(s) is(are) not homogeneously distributed within the 3D supporting matrix[31]. In fact, the first bioreactor system using bi-axial rotational stimulation to improve the outcome of 3D cell culture was a rotating vessel where all the specimens are inserted in a single culture condition[32]. However, there are no bioreactors adapted for bilayered scaffolds or heterotypic cultures that provide different culture media for each layer in a single chamber, allowing inducing rotatory stimulus, such as bi-axial (horizontal and vertical) movements to avoid cell sedimentation and stimulate tissue formation, at the same time. All these features were combined and demonstrated, computationally and experimentally, in the present work.

A 3D PCL scaffold was prototyped to support the experimental and numerical modulation. The numerical simulation of the cell seeding was performed with particles of 25 μm diameter. Human cells broadly vary from 4 to 39 μm. Taking into consideration that the simulated and prototyped scaffold have pores of 500 μm, the cell seeding performance was not expected to change for cells with diameter around the 25 μm of the simulated spherical particles. Mostly, fibroblasts (16 μm), Hela cells (18 μm), osteoblasts (20 μm), alveolar macrophages (21 μm), and cardiomyocytes (31 μm) are within this range, for which the present numerical simulation is expected to be accurate[33], making the modeling able to be expanded to different cell types.

The mixture of two different culture conditions in the top and bottom compartments of the dual-chamber was only happening through the scaffold porosity. The rotational movements aimed at improving diffusive exchanges, i.e. nutrient uptake and cellular waste product removal, which was shown to improve metabolic activity and increase mRNA synthesis, while enabled the control over cell distribution.

Furthermore, the vertical and horizontal rotations are native in any articulated organism, which were precisely controlled by the developed bioreactor device. The induced horizontal rotation showed an increase of metabolic active cells compared with the static conditions, and higher RNA transcription activity, while the vertical one allowed a better cell distribution.

At last, as an evolution from a prototyped scaffold and a spongy-like hydrogel, the system was tested with a membrane interfacing a hydrogel. As a proof of concept, a BBB model was engineered, where two different culture conditions were established. Thus, a heterotypic culture was performed using a co-culture of cells, namely endothelial cells

Accepted Manuscript

adjacent to neural/epithelial ones in 3D, or even a mix of endothelial and mesenchymal cells adjacent to the neural/epithelial ones. Although the native BBB is composed by three types of cells: the brain microvascular endothelia cells, pericyte cells and the astrocytes, in close contact with neurons, in the present study brain microvascular endothelia cells were replaced by another type of microvascular cells, the hCoMECs, and the CD146+ hASCs mimicked the pericytes. The SH-SY5Y were used to introduce a multiple phenotypic lineage that could resemble the heterogeneous population of the neural side of the BBB. This cell line has adherent and floating cells, which were both kept in culture to produce the *in vitro* model, including this way neuroblast- and epithelial-like cells in the neural environment [20]. The rotational movements are also of importance to mimic the tissues, such as the brain, which is not only 3D nor under perfusion, but also under motion. Furthermore, as previously demonstrated in the present work, the rotational stimuli improve nutrient diffusion and cell metabolic activity in 3D.

The formation of the endothelial barrier was studied for its permeability using the flow of a fluorescent marker (Dextran 70 kDa), which is known to do not cross the human BBB[23]. While the global cell number was kept constant in the BBB-like membrane in both conditions, the co-culture significantly changed cell confluency and permeability. An important factor that may impact these characteristics is the presence of CD146+ hASCs, promoting the connection to endothelial cells by N-cadherin, which has been implicated in regulation of Trio, a RhoA/Rac1 GTPase activation protein (GAP) that controls the native BBB stability[34]. In a previous study, pericyte-deficient mice was shown to have abnormal leakage in the central nervous system due to increased transcytosis and perhaps other endothelial cell defects[35], corroborating the important synergy of both cell types when modelling the BBB. Strikingly, a reduction in pericyte number can cause a loss of tight junctions between endothelial cells, leading to increased BBB permeability, as herein observed. The absence of CD146+ hASCs negatively impacted the membrane confluency and increased its permeability to Dextran 70 kDa. This phenotypic disorder in the BBB is also a biomarker during the development of Alzheimer's disease, as previously reported by Sengillo *et al* [36]. These aspects are of relevant consideration for future studies using the herein described model.

In the future, the bioreactor has the potential to be used to develop other dynamic 3D *in vitro* models of interfaced tissues. Further studies on the herein disclosed BBB model may be developed to better understand the role of the different cells in the function of the engineered

Accepted Manuscript

tissue, particularly on its permeability. Furthermore, due to the growing interest in mechanotransduction as a method to control cell behavior and stem cell differentiation, the presented system enables a new stimulation mechanism currently under-studied. Then, further studies involving the effect of different rotational speeds and absence of gravity should be investigated, with particular interest for 3D cell cultures, constructs, and organoids.

5. Conclusion

In summary, the development of a bioreactor system and its characterization, through mathematical and experimental modulation, were performed in the present work. A dynamic platform with a user-friendly control – vertical and horizontal rotations for an improved medium diffusion and cell homogenization – was created. The bioreactor was used to validate a predictive mathematical modelling of cell seeding and nutrient mixing in 3D cultures. The effect of the vertical and horizontal rotations over cell seeding, metabolic and RNA transcription activity were characterized, showing the control over cell distribution and improved cell viability. The design of attachable dual-chambers enables the perfusion of two different culture conditions in interconnected compartments. Having successfully supported a range of cellular supports and environments, the cell culture platform versatility and utility was corroborated. The simulation and experimental results demonstrated the creation of a top, interface (gradient), and bottom biochemical regions which controlled specific tissue phenotypes in a single environment. Finally, the system was experimentally tested for the engineering of an artificial BBB, being of interest for further applications involving 3D cell culture, TE strategies, tissue modelling, and drug testing.

Accepted Manuscript

Data availability

The data that support the findings of this study are available upon reasonable request from the authors.

Supporting Information

Supplementary methods (bioreactor design and control).

Supplementary results (Cellulose membrane morphometric characterization. Surface marker CD146 quantification).

Supplementary videos (Projection of the working bioreactor. Video of the device working inside an incubator).

Acknowledgement

The authors are thankful for the Portuguese Foundation for Science and Technology (FCT) distinction attributed to R. F. Canadas (SFRH/BD/92565/2013). R. F. Canadas is also thankful to FCT, Fundo Europeu de Desenvolvimento Regional (FEDER), and Programa Operacional Competitividade e Internacionalização (POCI) for funding the B-Liver Project (PTDC/EMD-EMD/29139/2017) and for the funds provided under the 3BioMeD project (JICAM/0001/2017). The authors would like to acknowledge the financial support of European Union via H2020-MSCA-RISE program (BAMOS, grant number 734156], and the support of the Innovative UK via Newton Fund [grant number 102872].

Accepted Manuscript

References

[1] Zohar B, Blinder Y, Epshtein M, Szklanny A A, Kaplan B, Korin N, Mooney D J and Levenberg S 2019 Multi-flow channel bioreactor enables real-time monitoring of cellular dynamics in 3D engineered tissue *Commun. Biol.* **2** 158

[2] Lovecchio J, Gargiulo P, Vargas Luna J L, Giordano E and Sigurjónsson Ó E 2019 A standalone bioreactor system to deliver compressive load under perfusion flow to hBMSC-seeded 3D chitosan-graphene templates *Sci. Rep.* **9** 16854

[3] O'Brien F J 2011 Biomaterials & scaffolds for tissue engineering *Mater. Today* **14** 88–95

[4] Caddeo S, Boffito M and Sartori S 2017 Tissue Engineering Approaches in the Design of Healthy and Pathological In Vitro Tissue Models *Front. Bioeng. Biotechnol.* **5** 40

[5] Dang M, Saunders L, Niu X, Fan Y and Ma P X 2018 Biomimetic delivery of signals for bone tissue engineering *Bone Res.* **6** 25

[6] Schmid J, Schwarz S, Meier-Staude R, Sudhop S, Clausen-Schaumann H, Schieker M and Huber R 2018 A Perfusion Bioreactor System for Cell Seeding and Oxygen-Controlled Cultivation of Three-Dimensional Cell Cultures *Tissue Eng. Part C. Methods* **24** 585–95

[7] Tandon N, Marolt D, Cimetta E and Vunjak-Novakovic G 2013 Bioreactor engineering of stem cell environments *Biotechnol. Adv.* **31** 1020–31

[8] Panchalingam K M, Jung S, Rosenberg L and Behie L A 2015 Bioprocessing strategies for the large-scale production of human mesenchymal stem cells: a review *Stem Cell Res. Ther.* **6** 225

[9] Canadas R F, Ren T, Marques A P, Oliveira J M, Reis R L and Demirci U 2018 Biochemical Gradients to Generate 3D Heterotypic-Like Tissues with Isotropic and Anisotropic Architectures *Adv. Funct. Mater.* **0** 1804148

[10] Vunjak-Novakovic G, Freed L E, Biron R J and Langer R 1996 Effects of mixing on the composition and morphology of tissue-engineered cartilage *AIChE J.* **42** 850–60

[11] Freed L E and Vunjak-Novakovic G 1997 Microgravity tissue engineering *Vitr. Cell.*

Accepted Manuscript

Dev. Biol. - Anim. **33** 381–5

[12] Carrier R L, Rupnick M, Langer R, Schoen F J, Freed L E and Vunjak-Novakovic G 2002 Perfusion Improves Tissue Architecture of Engineered Cardiac Muscle *Tissue Eng.* **8** 175–88

[13] Altman G H, Horan R L, Martin I, Farhadi J, Stark P R H, Volloch V, Richmond J C, Vunjak-Novakovic G and Kaplan D L 2001 Cell differentiation by mechanical stress *FASEB J.*

[14] Chen D, Wu J Y, Kennedy K M, Yeager K, Bernhard J C, Ng J J, Zimmerman B K, Robinson S, Durney K M, Shaeffer C, Vila O F, Takawira C, Gimble J M, Guo X E, Ateshian G A, Lopez M J, Eisig S B and Vunjak-Novakovic G 2020 Tissue engineered autologous cartilage-bone grafts for temporomandibular joint regeneration *Sci. Transl. Med.* **12** eabb6683

[15] Carvalho M R, Barata D, Teixeira L M, Giselbrecht S, Reis R L, Oliveira J M, Truckenmüller R and Habibovic P 2019 Colorectal tumor-on-a-chip system: A 3D tool for precision onco-nanomedicine *Sci. Adv.* **5** eaaw1317

[16] Liu Z, Tamaddon M, Gu Y, Yu J, Xu N, Gang F, Sun X and Liu C 2020 Cell Seeding Process Experiment and Simulation on Three-Dimensional Polyhedron and Cross-Link Design Scaffolds. *Front. Bioeng. Biotechnol.* **8** 104

[17] Andjelkovic A V, Stamatovic S M, Phillips C M, Martinez-Revollar G and Keep R F 2020 Modeling blood–brain barrier pathology in cerebrovascular disease in vitro: current and future paradigms *Fluids Barriers CNS* **17** 44

[18] Liu Z, Tao C, Yuan S, Wang W, Tamaddon M, Ng L, Huang H, Sun X and Liu C 2021 Eularian wall film model for predicting dynamic cell culture process to evaluate scaffold design in a perfusion bioreactor *Med. Nov. Technol. Devices* 100104

[19] Liu Z, Tamaddon M, Chen S-M, Wang H, San Cheong V, Gang F, Sun X and Liu C 2021 Determination of an Initial Stage of the Bone Tissue Ingrowth Into Titanium Matrix by Cell Adhesion Model *Front. Bioeng. Biotechnol.* **9** 736063

[20] Kovalevich J and Langford D 2013 Considerations for the use of SH-SY5Y neuroblastoma cells in neurobiology *Methods Mol. Biol.* **1078** 9–21

[21] Hawkins R A, Phelps M E, Huang S-C, Wapenski J A, Grimm P D, Parker R G,

Accepted Manuscript

Juillard G and Greenberg P 1984 A Kinetic Evaluation of Blood—Brain Barrier Permeability in Human Brain Tumors with [68Ga]EDTA and Positron Computed Tomography *J. Cereb. Blood Flow Metab.* **4** 507–15

[22] Mendes L F, Pirraco R P, Szymczyk W, Frias A M, Santos T C, Reis R L and Marques A P 2012 Perivascular-like cells contribute to the stability of the vascular network of osteogenic tissue formed from cell sheet-based constructs. *PLoS One* **7** e41051

[23] Pardridge W M Blood-Brain Barrier Drug Targeting Enables Neuroprotection in Brain Ischemia Following Delayed Intravenous Administration of Neurotrophins *Madame Curie Biosci. Database*

[24] Schindelin J, Arganda-Carreras I, Frise E, Kaynig V, Longair M, Pietzsch T, Preibisch S, Rueden C, Saalfeld S, Schmid B, Tinevez J-Y, White D J, Hartenstein V, Eliceiri K, Tomancak P and Cardona A 2012 Fiji: an open-source platform for biological-image analysis *Nat. Methods* **9** 676

[25] Wendt D, Marsano A, Jakob M, Heberer M and Martin I 2003 Oscillating perfusion of cell suspensions through three-dimensional scaffolds enhances cell seeding efficiency and uniformity *Biotechnol. Bioeng.* **84** 205–14

[26] Chang C-H, Lin F-H, Lin C-C, Chou C-H and Liu H-C 2004 Cartilage tissue engineering on the surface of a novel gelatin–calcium-phosphate biphasic scaffold in a double-chamber bioreactor *J. Biomed. Mater. Res. Part B Appl. Biomater.* **71B** 313–21

[27] Smith T J N, Peracic M R, Pugh S M, Hagg R, Tommasini R, Larcher Y and Misner L D 2005 Automated tissue engineering system

[28] Hutmacher D W, Teoh S H, Ranawake M, Chong W S, Ting K S, Chua K C, Myint T, Puah C M, Foo T T and Jan-Thorsten S 2006 Bioreactor for growing cell or tissue cultures

[29] Taboas J M, Tuan R S and Hudson S D 2006 Bioreactor Device, And Method And System For Fabricating Tissues In The Bioreactor Device

[30] Moretti M G, Freed L E and Langer R S 2008 Oscillating Cell Culture Bioreactor

[31] Chen X, Zhang L, Yang X, Li Z, Sun X, Lin M, Yang G and Gou Z 2013 Micronutrients-incorporated calcium phosphate particles with protective effect on

Accepted Manuscript

osteoporotic bone tissue. *J. Nutr. Health Aging* **17** 426–33

[32] Zhang Z-Y, Teoh S H, Chong W-S, Foo T-T, Chng Y-C, Choolani M and Chan J 2009 A biaxial rotating bioreactor for the culture of fetal mesenchymal stem cells for bone tissue engineering *Biomaterials* **30** 2694–704

[33] Milo R, Jorgensen P, Moran U, Weber G and Springer M 2010 BioNumbers - the database of key numbers in molecular and cell biology *Nucleic Acids Res.* **38** D750–3

[34] Kruse K, Lee Q S, Sun Y, Klomp J, Yang X, Huang F, Sun M Y, Zhao S, Hong Z, Vogel S M, Shin J-W, Leckband D E, Tai L M, Malik A B and Komarova Y A 2018 N-cadherin signaling via Trio assembles adherens junctions to restrict endothelial permeability *J. Cell Biol.* **218** 299–316

[35] Armulik A, Genové G, Mäe M, Nisancioglu M H, Wallgard E, Niaudet C, He L, Norlin J, Lindblom P, Strittmatter K, Johansson B R and Betsholtz C 2010 Pericytes regulate the blood–brain barrier *Nature* **468** 557–61

[36] Sengillo J D, Winkler E A, Walker C T, Sullivan J S, Johnson M and Zlokovic B V 2013 Deficiency in mural vascular cells coincides with blood-brain barrier disruption in Alzheimer's disease *Brain Pathol.* **23** 303–10

Accepted Manuscript